

# Thermal entanglement in fully connected spin systems and its RPA description

J.M. Matera, R. Rossignoli, N. Canosa

*Departamento de Física-IFLP, Universidad Nacional de La Plata, C.C.67, La Plata (1900), Argentina*

We examine the thermal pairwise entanglement in a symmetric system of  $n$  spins fully connected through anisotropic  $XYZ$ -type couplings embedded in a transverse magnetic field. We consider both the exact evaluation together with that obtained with the static path + random phase approximation (RPA) and the ensuing mean field + RPA. The latter is shown to provide an accurate analytic description of both the parallel and antiparallel thermal concurrence in large systems. We also analyze the limit temperature for pairwise entanglement, which is shown to increase for large fields and to decrease logarithmically with increasing  $n$ . Special finite size effects are as well discussed.

PACS numbers: 03.67.Mn, 03.65.Ud, 75.10.Jm

## I. INTRODUCTION

Quantum entanglement, one of the most fundamental and intriguing features of quantum mechanics, is well recognized as an essential resource for quantum information processing and transmission [1–3]. It has recently acquired an important role also in many-body and condensed matter physics [4–7], where it provides a new perspective for analyzing quantum correlations and quantum phase transitions, as well as in other fields like the foundations of statistical mechanics [8]. The study of entanglement in interacting spin models has in particular attracted much interest [4–7, 9–17], since they provide a basic scalable qubit representation suitable for implementing quantum processing tasks and are at the same time able to capture the main features of diverse physical systems. Some of these models can in addition be exactly solved for any size, providing hence a suitable scenario for testing the accuracy of approximate descriptions.

An example is that of a symmetric array of  $n$  fully connected spins (simplex) with anisotropic  $XYZ$  type couplings embedded in a uniform transverse magnetic field. This is a solvable yet non-trivial model which exhibits a quantum phase transition at  $T = 0$ , whose Hamiltonian is formally equivalent to that of the well-known Lipkin-Meshkov-Glick (LMG) model [18]. It has attracted renewed interest in recent years, having been used to describe diverse physical systems such as Josephson junction arrays [19] and two mode Bose Einstein condensates [20]. Its zero temperature entanglement properties were analyzed in detail in refs. [12–15], where it was shown in particular that the pairwise concurrence, a measure of the entanglement between two spins [21], exhibited a rich behavior when properly scaled, with a cusplike maximum at the critical field in the ferromagnetic case and a smooth decrease for large fields [14].

In this work we will examine the *thermal* pairwise entanglement in this system, together with its description in the framework of the mean field + random phase approximation (RPA) derived from the path integral representation of the partition function [22, 23]. Our aim is twofold. First, we want to determine its thermal behavior and stability, a relevant aspect in physical real-

izations. Secondly, given the complexity of determining the entanglement properties in general interacting many-body systems at finite temperature, we want to examine the extent to which its main features can be captured by a general tractable method like the RPA, which takes into account just small amplitude quantum fluctuations around the mean field. We will show that the present RPA treatment provides, for anisotropic couplings, an accurate analytic description of both the parallel and antiparallel thermal pairwise entanglement in large systems, generalizing the results of [23] for the  $XXZ$  case (where entanglement is just antiparallel). The limit temperature will be shown to decrease only logarithmically with increasing  $n$  at all fields, for the standard  $1/n$  scaling of coupling strengths, and to exhibit a different field dependence in the parallel and antiparallel sectors. In particular, it *increases* for large increasing fields, despite the decrease of the  $T = 0$  concurrence (and at variance with the behavior in the  $XXZ$  case [23]), entailing just a finite separable field window at any temperature.

Section II describes the model and its exact partition function and concurrence, together with their evaluation in the static path and mean field + RPA treatments and the asymptotic expressions. Section III discusses in detail the exact numerical and approximate results in finite systems. Finally, conclusions are drawn in IV.

## II. FORMALISM

### A. Exact partition function and concurrence

We will consider  $n$  qubits or spins  $1/2$  coupled through an anisotropic full range  $XYZ$  Heisenberg interaction in a transverse magnetic field  $b$ . The Hamiltonian reads

$$\begin{aligned} H &= b \sum_{i=1}^n s_i^z - \frac{1}{n} \sum_{i \neq j}^n (v_x s_x^i s_x^j + v_y s_y^i s_y^j + v_z s_z^i s_z^j) \\ &= b S_z - \frac{1}{n} \sum_{\mu=x,y,z} v_\mu (S_\mu^2 - \frac{n}{4}), \end{aligned} \quad (1)$$

where  $s_\mu^i$  denotes the spin component at site  $i$  (in units of  $\hbar$ ) and  $S_\mu = \sum_{i=1}^n s_\mu^i$  the total spin components. The  $1/n$

scaling of coupling strengths ensures that all intensive energies remain finite for  $n \rightarrow \infty$  and finite  $v_\mu$ . For  $T > 0$  the total spin  $S^2 = \sum_\mu S_\mu^2$  is no longer fixed, so that all terms in (1) are independent. Nonetheless, without loss of generality we can assume  $|v_y| \leq |v_x|$  and  $b \geq 0$ . We will consider here the attractive case  $v_x > 0$  (with  $|v_y| \leq v_x$ ) where the ground state will have maximum spin  $S = n/2$ .

Since  $H$  is completely symmetric and commutes with both  $S^2$  and the  $S_z$ -parity  $P = \exp[i\pi(S_z + n/2)]$  (global phaseflip) the partition function at temperature  $T = \beta^{-1}$  (we set Boltzmann constant  $k = 1$ ) can be written as

$$Z = \text{Tr} \exp[-\beta H] = \sum_{S=\delta_n}^{n/2} Y(S) \sum_{\nu=\pm, k} e^{-\beta E_{S k \nu}}, \quad (2)$$

where  $Y(S) = \binom{n}{n/2-S} - \binom{n}{n/2-S-1}$ , with  $Y(n/2) = 1$ , is the multiplicity of states with total spin  $S$ , such that  $\sum_{S=\delta_n}^{n/2} Y(S)(2S+1) = 2^n$  [ $\delta_n = 0$  ( $\frac{1}{2}$ ) for  $n$  even (odd)] and  $E_{S k \nu}$  are the eigenvalues of  $H$  with total spin  $S$  and parity  $\nu$  [ $k = 1, \dots, S + \frac{1}{2} + \nu(\frac{1}{2} - \delta_n)$ ]. It should be noticed that in the fermionic realization [18], the multiplicities  $Y(S)$  would be different (the total number of states in the half-filled fermionic system is  $\binom{2n}{n}$  instead of  $2^n$ ).

The pairwise entanglement at  $T > 0$  is determined by the reduced two-spin density matrix  $\rho_{ij} = \text{Tr}_{n-\{ij\}} \rho$  ( $i \neq j$ ), where  $\rho = Z^{-1} \exp[-\beta H]$  is the global thermal density.  $\rho_{ij}$  will be entangled if it cannot be written as a convex combination of product densities [24], i.e., if  $\rho_{ij} \neq \sum_\alpha q_\alpha \rho_i^\alpha \otimes \rho_j^\alpha$ , with  $q_\alpha > 0$ , being separable otherwise. The amount of pairwise entanglement can be measured through the entanglement of formation  $E_{ij}$  [25], which in the case of two qubits can be evaluated as [21]  $E_{ij} = -\sum_{\nu=\pm} q_\nu \log_2 q_\nu$ , with  $q_\pm = \frac{1}{2}(1 \pm \sqrt{1 - C_{ij}^2})$  and  $C_{ij}$  the *concurrence* [21], itself an entanglement measure [26]. Since  $E_{ij}$  is in this case just an increasing function of  $C_{ij}$ , with  $C_{ij} = E_{ij} = 1$  (0) for a maximally entangled (separable) pair, it is equivalent to use  $C_{ij}$  as measure.

In the present system  $\rho_{ij}$  will be the same for any pair and will commute with the reduced parity  $\exp[i\pi(s_z^i + s_z^j + 1)]$  and total spin  $\sum_\mu (s_\mu^i + s_\mu^j)^2$ , being in the standard basis of the form

$$\rho_{ij} = \begin{pmatrix} p_+ & 0 & 0 & \alpha_+ \\ 0 & p_0 & \alpha_- & 0 \\ 0 & \alpha_- & p_0 & 0 \\ \alpha_+ & 0 & 0 & p_- \end{pmatrix}, \quad \begin{aligned} \alpha_\pm &= \langle s_+^i s_\pm^j \rangle = \alpha_x \mp \alpha_y \\ p_\pm &= \frac{1}{4} + \alpha_z \pm \langle s_z \rangle \\ p_0 &= \frac{1}{4} - \alpha_z \end{aligned}$$

where  $s_\pm^i = s_x^i \pm i s_y^i$  and  $(\mu = x, y, z)$

$$\alpha_\mu \equiv \langle s_\mu^i s_\mu^j \rangle = \frac{T}{n-1} \frac{\partial \ln Z}{\partial v_\mu} \quad (i \neq j), \quad (3)$$

$$\langle s_z \rangle \equiv \langle s_z^i \rangle = -\frac{T}{n} \frac{\partial \ln Z}{\partial b}. \quad (4)$$

Note that  $-\frac{1}{4(n-1)} \leq \alpha_\mu \leq \frac{1}{4}$  as  $\langle S_\mu^2 \rangle = \frac{n}{4} + n(n-1)\alpha_\mu$ . The ensuing concurrence  $C \equiv C_{ij}$  can be expressed as

$C = \text{Max}[C_+, C_-, 0]$ , with

$$C_+ = 2(|\alpha_+| - p_0) = 2(\alpha_x - \alpha_y + \alpha_z - \frac{1}{4}), \quad (5)$$

$$C_- = 2(|\alpha_-| - \sqrt{p_+ p_-}) \\ = 2(\alpha_x + \alpha_y - \sqrt{(\frac{1}{4} + \alpha_z)^2 - \langle s_z \rangle^2}). \quad (6)$$

Here  $C_+$  ( $C_-$ ) denotes a concurrence of parallel (antiparallel) type [27], as in Bell states  $|\uparrow\uparrow\rangle \pm |\downarrow\downarrow\rangle$  ( $|\uparrow\downarrow\rangle \pm |\downarrow\uparrow\rangle$ ). Just one can be positive for a given  $\rho_{ij}$ . In the final expressions (5)–(6) we have assumed  $\alpha_\pm > 0$ , valid for the present attractive case  $v_x \geq |v_y|$ . Since all pairs are equally entangled, the maximum value that can be attained by  $C$  in the present system is  $2/n$  [28] (reached for instance in the  $W$ -state  $|SM\rangle = |\frac{n}{2}, \frac{n}{2} - 1\rangle$ ) implying that only the rescaled concurrence  $c = nC$  can remain finite in the thermodynamic limit  $n \rightarrow \infty$ .

## B. Static path + RPA

The auxiliary field path integral representation of the partition function (2) can be written as [22]

$$Z = \int D[\mathbf{r}] \text{Tr} \left[ \hat{T} \exp\{-\int_0^\beta H[\mathbf{r}(\tau)] d\tau\} \right], \quad (7)$$

$$H(\mathbf{r}) = b S_z - \mathbf{r} \cdot \mathbf{S} + \frac{1}{4} \sum_\mu (n \frac{r_\mu^2}{v_\mu} + v_\mu), \quad (8)$$

where  $\mathbf{r} = (x, y, z)$ ,  $\hat{T}$  denotes (imaginary) time ordering and  $H(\mathbf{r})$  represents a linearized Hamiltonian. Normalization  $\int D[\mathbf{r}] \exp[-\int_0^\beta \sum_\mu \frac{n r_\mu^2(\tau)}{4v_\mu} d\tau] = 1$  is assumed. Starting from a Fourier expansion  $\mathbf{r}(\tau) = \sum_{k=-\infty}^\infty \mathbf{r}_k e^{i\omega_k \tau}$ ,  $\omega_k = 2\pi k/\beta$ , with  $D[\mathbf{r}] \propto \prod_k d^3 \mathbf{r}_k$ , the static path + random phase approximation [29–31] [to be denoted as correlated SPA (CSPA)] preserves the full integral over the static components  $\mathbf{r} \equiv \mathbf{r}_0$  but integrates over  $\mathbf{r}_k$ ,  $k \neq 0$ , in the saddle point approximation, for each value of the running static variables. This procedure takes thus into account large amplitude static fluctuations, relevant in critical regions, together with small amplitude quantum fluctuations, and is feasible above a low breakdown temperature  $T^*$ . The final result for the present spin 1/2 system can be cast as

$$Z_{\text{CSPA}} = \sqrt{\prod_\mu \frac{n\beta}{4\pi v_\mu}} \int_{-\infty}^\infty Z(\mathbf{r}) \frac{\omega(\mathbf{r}) \sinh[\frac{1}{2}\beta\lambda(\mathbf{r})]}{\lambda(\mathbf{r}) \sinh[\frac{1}{2}\beta\omega(\mathbf{r})]} d^3 \mathbf{r}, \quad (9)$$

where, defining  $\boldsymbol{\lambda} = \mathbf{r} - \mathbf{b} = (x, y, z - b)$ ,

$$Z(\mathbf{r}) = \text{Tr} \exp[-\beta H(\mathbf{r})] \\ = e^{-\frac{1}{4}\beta \sum_\mu (n r_\mu^2 / v_\mu + v_\mu)} [2 \cosh \frac{1}{2}\beta\lambda(\mathbf{r})]^n, \quad (10)$$

$$\lambda(\mathbf{r}) = [\sum_\mu \lambda_\mu^2]^{1/2}, \quad (11)$$

$$\omega(\mathbf{r}) = [\sum_\mu \lambda_\mu^2 (1 - f_\mu)(1 - f_{\mu'})]^{1/2}, \quad (12)$$

$$f_\mu = v_\mu \tanh[\frac{1}{2}\beta\lambda(\mathbf{r})]/\lambda(\mathbf{r}), \quad (13)$$

with  $\mu' < \mu''$ ,  $\mu', \mu'' \neq \mu$ . In (9)  $Z(\mathbf{r})$  is a Hartree-like partition function while the remaining factor accounts for the small amplitude quantum corrections, with  $\omega(\mathbf{r})$  the single collective thermal RPA energy existing in the present system. It can be obtained from the equation

$$\text{Det}[\delta_{\mu\mu'} - 2v_\mu \sum_{\nu=\pm} s_\mu^\nu s_{\mu'}^{-\nu} \frac{p_{-\nu} - p_\nu}{\varepsilon_\nu - \varepsilon_{-\nu} - \omega}] = 0, \quad (14)$$

with  $s_\mu^\nu \equiv \langle \nu | s_\mu | -\nu \rangle$ ,  $p_\nu = e^{-\beta\varepsilon_\nu} / \sum_\nu e^{-\beta\varepsilon_\nu}$  and  $|\nu\rangle$ ,  $\varepsilon_\nu$  the eigenstates and eigenvalues of  $\boldsymbol{\lambda} \cdot \mathbf{s}$ . If  $v_\mu < 0$ , the corresponding integral should be done along the imaginary axes and can be evaluated in the saddle point approximation [31]. The elements (3)-(4) become

$$\alpha_\mu = \frac{1}{2(n-1)} \left\langle \frac{nr_\mu^2}{2v_\mu^2} - \frac{1}{\beta v_\mu} - \frac{1}{2} + \left( \frac{2}{\beta\omega} - \coth \frac{1}{2}\beta\omega \right) \frac{\partial\omega}{\partial v_\mu} \right\rangle$$

and  $\langle s_z \rangle = \frac{1}{2} \langle z \rangle / v_z$ , where  $\langle \dots \rangle$  denotes CSPA averages.

### C. Mean field + RPA

For sufficiently large  $n$  and away from the critical region, we may integrate all variables  $\mathbf{r}_k$ , including  $\mathbf{r}_0$ , in the saddle point approximation around the minimum of the free energy potential  $-T \ln Z(\mathbf{r})$ , determined by the self-consistent equations

$$r_\mu = f_\mu(r_\mu - b_\mu), \quad \mu = x, y, z. \quad (15)$$

This leads to the mean-field+RPA (MF+RPA). For an *isolated* minimum at  $\mathbf{r} = \mathbf{r}_0$ , we obtain

$$Z_{\text{MF+RPA}} = \frac{Z(\mathbf{r}_0) \sinh \frac{1}{2}\beta\lambda}{\sqrt{1-\zeta} \sinh \frac{1}{2}\beta\omega}, \quad (16)$$

where  $\zeta = 1 - \frac{\lambda^2}{\omega^2} \text{Det}[-\frac{2v_\mu}{n\beta} \frac{\partial^2 \ln Z(\mathbf{r})}{\partial r_\mu \partial r_{\mu'}}]_{\mathbf{r}_0}$  accounts for the gaussian static fluctuations and  $\lambda \equiv \lambda(\mathbf{r}_0)$ ,  $\omega \equiv \omega(\mathbf{r}_0)$ . In (16),  $Z(\mathbf{r}_0)$  is the MF partition function while the last factor is the proper RPA correction, which represents the ratio of two independent boson partition functions: that of bosons of energy  $\omega$  to that of bosons of energy  $\lambda$ .

For the present Hamiltonian Eqs. (15) imply either  $r_\mu = 0$  or  $f_\mu = 1$  for  $\mu = x, y$ . For  $|v_y| < v_x$  and  $v_z < v_x$ , we then obtain the following minima:

a) If  $|b| < b_c$  and  $T < T_c(b)$ , where

$$b_c = v_x - v_z, \quad T_c(b) = \frac{v_x b / b_c}{\ln \frac{1+b/b_c}{1-b/b_c}}, \quad (17)$$

the minimum corresponds to the degenerate *parity-breaking* solution  $\mathbf{r} = (\pm x, 0, z)$ , with  $x \neq 0$ . In this case  $\lambda$  is determined by the equation  $f_x = 1$ , i.e.,

$$\lambda = v_x \tanh \frac{1}{2}\beta\lambda, \quad (18)$$

which depends just on  $v_x$  and  $T$  ( $\lambda = v_x$  at  $T = 0$ ), while  $z = -v_z b / b_c$  (independent of  $T$ ) and  $x = \sqrt{\lambda^2 - v_x^2 b^2 / b_c^2}$ ,

the constraint  $\lambda > v_x b / b_c$  leading to Eq. (17). At this solution, the RPA energy (12) becomes

$$\omega = x \sqrt{(1-f_y)(1-f_z)}, \quad (19)$$

with  $f_\mu = v_\mu / v_x$ , while  $\zeta = \frac{1}{2}\beta v_x / \cosh^2 \frac{1}{2}\beta\lambda$ . Note that  $\omega \rightarrow 0$  for  $T \rightarrow T_c(b)$  (as  $x \rightarrow 0$ ) or  $v_y \rightarrow v_x$  (as  $f_y \rightarrow 1$ ), implying the divergence of (16) in these limits (see [23] for the correct MF+RPA treatment in the continuously degenerate XXZ case).

b) For  $|b| > b_c$  or  $T > T_c(b)$ , the minimum corresponds to the *normal* solution  $\mathbf{r} = (0, 0, z)$ . In this case  $\lambda = b - z$  is the positive root of the equation

$$\lambda = b + v_z \tanh \frac{1}{2}\beta\lambda \quad (20)$$

with  $\lambda = b + v_z$  at  $T = 0$ . The RPA energy becomes

$$\omega = \lambda \sqrt{(1-f_x)(1-f_y)}. \quad (21)$$

with  $f_\mu = (1 - b/\lambda)v_\mu / v_z$ , while  $\zeta = \frac{1}{2}\beta v_z / \cosh^2 \frac{1}{2}\beta\lambda$ . Here  $\omega \rightarrow 0$  for  $T \rightarrow T_c(b)$  (as  $f_x \rightarrow 1$ ) but remains finite for  $v_y \rightarrow v_x$ . This is also the only solution for  $v_z > v_x$ .

The ensuing expressions for the elements (3)-(4) are

$$\alpha_\mu = \frac{1}{2(n-1)} \left( \frac{nr_\mu^2}{2v_\mu^2} - \frac{1}{2} + \delta_{v_\mu} \right), \quad \langle s_z \rangle = \frac{1}{2n} \left( \frac{nz}{v_z} + \delta_b \right),$$

$$\delta_\eta \equiv \frac{\partial\lambda}{\partial\eta} \coth \frac{1}{2}\beta\lambda - \frac{\partial\omega}{\partial\eta} \coth \frac{1}{2}\beta\omega + \frac{T}{1-\zeta} \frac{\partial\zeta}{\partial\eta},$$

with  $\eta = v_\mu, b$ . The first term in  $\alpha_\mu$ ,  $\langle s_z \rangle$  is the  $O(1)$  Hartree contribution, whereas  $\delta_\eta$  provides the  $O(1/n)$  RPA corrections, essential for describing entanglement.

### D. Asymptotic expressions for the concurrence

Full expressions for the MF+RPA concurrence are rather long and are given in the Appendix. However, up to  $O(1/n)$  terms and for sufficiently low  $T$ , we obtain

$$C_+ \approx \frac{1}{n-1} \left( 1 - \frac{\omega}{v_x - v_y} \coth \frac{1}{2}\beta\omega \right) - 2e^{-\beta v_x}, \quad (22)$$

$$C_- \approx \frac{1}{n-1} \left( 1 - \frac{v_x - v_y}{\omega} \coth \frac{1}{2}\beta\omega \right) - 2e^{-\beta v_x} \quad (23)$$

in the symmetry-breaking phase ( $|b| < b_c$ ), where

$$\frac{\omega}{v_x - v_y} = \sqrt{\frac{1 - (b/b_c)^2}{1 - \chi}}, \quad \chi = \frac{v_y - v_z}{v_x - v_z}, \quad (24)$$

whereas in the normal phase ( $b > b_c$ ),  $C_- \leq 0$  while

$$C_+ = \frac{1}{n-1} \left( 1 - \frac{\omega}{b + v_z - v_y} \coth \frac{1}{2}\beta\omega \right) - 2e^{-\beta(b+v_z)} \quad (25)$$

with

$$\frac{\omega}{b + v_z - v_y} = \sqrt{\frac{b/b_c - 1}{b/b_c - \chi}}. \quad (26)$$

We have used in (22)–(26) the  $T = 0$  values for  $\lambda$  and  $\omega$ , as the ensuing thermal corrections will be of order  $e^{-\beta\lambda} = O(1/n)$  for temperatures where (22), (23) and (25) are positive, leading then to  $O(1/n^2)$  terms in  $C$ . Eqs. (22)–(25) become increasingly accurate as  $n$  increases (coinciding for  $T \rightarrow 0$  and  $v_z = 0$  with the expressions of ref. [14]) and can be summarized as

$$C_{\pm} \approx \frac{1 - (\frac{\omega}{\lambda - v_y})^{\pm 1} \coth \frac{1}{2}\beta\omega}{n - 1} - 2e^{-\beta\lambda}, \quad (27)$$

with  $\lambda = v_x$ ,  $\omega = \sqrt{(1 - b^2/b_c^2)(\lambda - v_y)(\lambda - v_z)}$  for  $|b| < b_c$  and  $\lambda = b + v_z$ ,  $\omega = \sqrt{(\lambda - v_x)(\lambda - v_y)}$  for  $b > b_c$ , the result for  $b > b_c$  applying just for  $C_+$ .

For  $T \rightarrow 0$  ( $e^{-\beta\lambda} \rightarrow 0$ ,  $\coth \frac{1}{2}\beta\omega \rightarrow 1$ )  $C_{\pm}$  is then fully determined for large  $n$  by the scaled field  $b/b_c$  and the anisotropy  $\chi$ . For  $0 < \chi < 1$  (i.e.,  $v_z < v_y < v_x$ ),  $C_-$  ( $C_+$ ) will be positive for  $|b| < b_s$  ( $> b_s$ ), where

$$b_s = b_c \sqrt{\chi}, \quad (28)$$

is the *factorizing field* [14, 32], where the system possesses a *separable* ground state. Accordingly, at  $T = 0$  both  $C_{\pm}$  *vanish* at  $b = b_s$ ,  $C$  being antiparallel for  $|b| < b_s$  and parallel for  $|b| > b_s$ . On the other hand, if  $\chi \leq 0$  ( $v_y \leq v_z < v_x$ ) or  $\chi > 1$  ( $v_y < v_x < v_z$ , in which case there is no symmetry-breaking phase)  $C$  is always parallel at  $T = 0$ . It is also seen from (25)–(26) that at  $T = 0$ ,  $C_+$  remains positive for arbitrarily large fields, with  $(n - 1)C_+ \approx \frac{1}{2}(1 - \chi)b_c/b$  for  $b \gg b_c$ .

*Thermal effects:* Away from  $b_c$  and the  $XXZ$  limit, the main thermal effect in Eqs. (22)–(25) will arise from the exponential term  $-2e^{-\beta\lambda}$ , which stems in MF+RPA from the Hartree contribution to  $\alpha_{\mu}$  and  $\langle s_z \rangle$  ( $\approx \frac{1}{4}T_{\mu}^2/v_{\mu}^2$  and  $\frac{1}{2}z/v_z$ ; if just this contribution is kept, Eqs. (5)–(6) lead to  $C_{\pm} \approx \frac{1}{2}(\tanh^2 \frac{1}{2}\beta\lambda - 1) \approx -2e^{-\beta\lambda}$  for  $\beta\lambda \gg 1$ ). It represents the effect of the temperature induced decrease of the total spin average  $\langle S^2 \rangle \approx \frac{1}{4}n^2 \tanh^2 \beta\lambda/2$ . In the exact result it arises from the lowest state of the  $S = n/2 - 1$  multiplet, which has excitation energy  $\approx \lambda$  (see Fig. 4 in next section) and multiplicity  $n - 1$  in Eq. (2).

The RPA thermal factor  $\coth \frac{1}{2}\beta\omega$  cannot, however, be neglected (i.e., replaced by 1) in (22)–(25), particularly for  $b$  close to  $b_c$  or  $\chi$  close to 1, as  $\omega$  is lower than  $\lambda$  (for  $v_{\mu} > 0$ ) and vanishes for  $b \rightarrow b_c$  or  $v_y \rightarrow v_x$ . In the exact result it represents essentially the effect of the excited states *within* the  $S = n/2$  multiplet, whose excitation energies have an approximate harmonic behavior (i.e.,  $\Delta E \approx k\omega$ ,  $k = 0, 1, \dots$ ; see Fig. 4). With this factor, Eq. (23) correctly reduces for  $v_y \rightarrow v_x$  and up to  $O(1/n)$  terms, to the asymptotic result for the  $XXZ$  case [23],

$$C_- \approx \frac{1}{n - 1} \left( 1 - \frac{2T/b_c}{1 - (b/b_c)^2} \right) - 2e^{-\beta v_x}, \quad (v_x = v_y) \quad (29)$$

while for  $b \rightarrow b_c$ , Eqs. (22) and (25) converge to

$$C_+ \approx \frac{1}{n - 1} \left( 1 - \frac{2T}{v_x - v_y} \right) - 2e^{-\beta v_x}, \quad (b = b_c). \quad (30)$$

Hence, in these regions the concurrence will initially exhibit an almost *linear* decrease with increasing  $T$  before the exponential term becomes appreciable, as a consequence of the low excitation energy of the  $S = n/2$  states.

In any case, for sufficiently large  $n$ , the concurrence will decrease monotonously with increasing  $T$ , with  $C_{\pm}$  vanishing at a limit temperature  $T_L^{\pm}$  that will decrease *logarithmically* with increasing  $n$ , as implied by Eq. (27):

$$T_L^{\pm} \approx \frac{\lambda}{\ln \frac{2(n-1)}{1 - (\frac{\omega}{\lambda - v_y})^{\pm 1} \coth \frac{1}{2}\beta\omega}}, \quad (31)$$

which is actually a transcendental equation for  $T_L^{\pm}$ . Both  $T_L^{\pm}$  vanish (logarithmically) for  $b \rightarrow b_s^{\pm}$ , with  $T_L^-$  decreasing and  $T_L^+$  increasing with increasing field (and  $T_L^+(b)$  developing a slope discontinuity at  $b_c$ ). The increase of  $T_L^+$  with increasing  $b$  *persists* for  $b \gg b_c$ , where

$$T_L^+ \approx \frac{b + v_z}{\ln \frac{4(n-1)b/b_c}{1 - \chi}}, \quad (32)$$

implying that at any fixed  $T$  parallel entanglement can be induced by increasing the field (for  $b \gg b_c$ ,  $\lambda$  and  $\omega$  become proportional to  $b$ , the system approaching then the entangled ground state as  $b$  increases). The same behavior was observed in the limit temperatures for non-zero global negativities in small anisotropic systems [17].

At fixed low  $T$ , the main thermal effect for  $0 < \chi < 1$  is thus the appearance of a *separable window*  $b_L^- \leq |b| \leq b_L^+$  (instead of a separable point) where  $C_{\pm} = 0$ , with

$$b_L^{\pm} \approx b_c \sqrt{1 - (1 - \chi)[\tanh \frac{1}{2}\beta\omega(1 - 2(n - 1)e^{-\beta v_x})]^{\pm 2}} \quad (33)$$

(valid for  $T < T_L^+(b_c)$  for  $b_L^+$  and  $T < T_L^-(0)$  for  $b_L^-$ ). Its width increases then with increasing  $n$  or  $T$ , with  $b_L^{\pm} \approx b_s[1 \pm 2(\chi^{-1} - 1)(n - 1)e^{-\beta v_x}]$  for  $ne^{-\beta v_x} \ll 1$ . For  $T > T_L^-(0)$  the separable window will extend through  $b = 0$  ( $C_{\pm} = 0$  for  $|b| < b_L^+$ ).

### III. COMPARISON WITH EXACT RESULTS IN FINITE SYSTEMS

Typical results for the magnetic behavior of the concurrence at finite temperatures are shown in Fig. 1 for the  $XY$  case ( $v_z = 0$ ) with  $n = 100$  spins and different anisotropies. It is first seen that MF+RPA results obtained with the asymptotic expressions (22)–(25) are very accurate except in the vicinity of the critical field, improving as  $T$  increases. The full CSPA results further improve those of the MF+RPA in the critical region for not too low  $T$ , being practically undistinguishable from the exact ones at the finite temperatures considered.

The top panel corresponds to the Ising case  $v_y = 0$ , where the concurrence is always parallel. At  $T = 0$  it smoothly increases from 0 as  $b$  increases, having a maximum near  $b_c$ , while for  $T > 0$  it becomes non-zero only

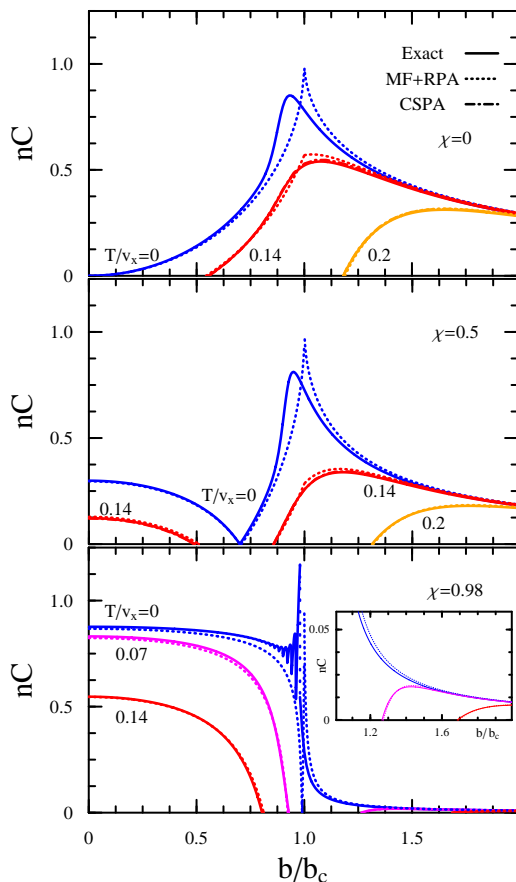


FIG. 1. (Color online) Scaled concurrence as a function of the magnetic field  $b$  for  $n = 100$  spins coupled through a full range  $XY$  interaction with anisotropies  $\chi = v_y/v_x = 0$  (top), 0.5 (center) and 0.98 (bottom), at different temperatures. Exact and asymptotic mean field+RPA (Eqs. (22)–(25)) results are depicted, together with those of CSPA (Eq. 9) for  $T > 0$  (almost undistinguishable from the exact ones).  $C$  is parallel (antiparallel) for  $b > b_s$  ( $< b_s$ ), with  $b_s$  the factorizing field (28). The inset depicts the (parallel) concurrence reentry for  $b > b_c$  at  $\chi = 0.98$ .

above a *threshold* field  $b_L^+$  (Eq. (33) for  $T < T_L^+(b_c)$ ). In the central panel ( $\chi = 0.5$ ) we may appreciate the vanishing of the concurrence at the factorizing field  $b_s \approx 0.71v_x$  at  $T = 0$ , where it changes from antiparallel to parallel. This point evolves into a separable window as  $T$  increases, which extends through  $b = 0$  for  $T > T_L^-(0) \approx 0.15v_x$ .

The bottom panel depicts the behavior close to the  $XXZ$  limit. In this case the exact  $T = 0$  concurrence  $C_-$  displays an oscillatory behavior as  $b \rightarrow b_s$  from below, as in the  $XXZ$  chain [23], which reflects the ground state spin parity transitions and which is not reproduced by MF+RPA (see however discussion of Fig. 5). Nonetheless, as  $T$  increases the oscillations become rapidly washed out and the asymptotic MF+RPA result becomes again accurate, correctly reproducing the exact concurrence at  $T/v_x = 0.07$  and 0.14, *including* the reentry of the parallel concurrence that takes place for high

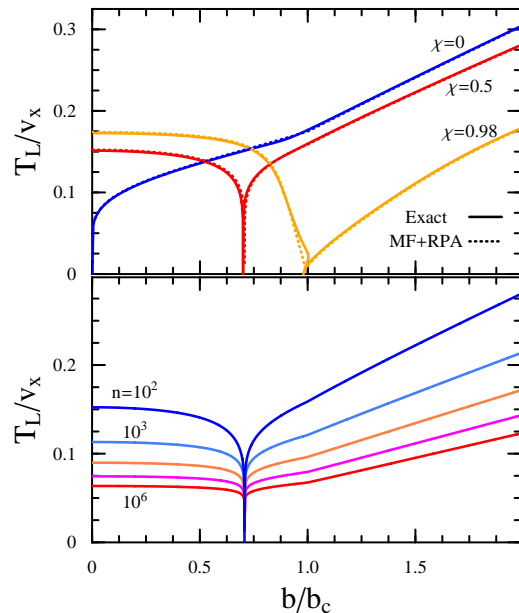


FIG. 2. (Color online) Top: Limit temperatures for pairwise entanglement  $T_L$  as a function of the magnetic field  $b$  for  $n = 100$  spins at the same anisotropies of Fig. 1, according to exact and MF+RPA results (Eq. (31)). They vanish at the factorizing field  $b_s$ . Regions below the limit temperature have finite pairwise entanglement, of antiparallel (parallel) type if  $b < b_s$  ( $> b_s$ ). Bottom: Limit temperatures for increasing number of spins at  $\chi = 0.5$  ( $n = 10^k$ ,  $k = 2, \dots, 6$ ).

fields. The thermal RPA factor  $\coth \frac{1}{2}\beta\omega$  is here essential for the accuracy as  $\beta\omega$  is small ( $\omega/v_x \lesssim 0.14$  for  $b < b_c$ ).

Let us mention that for  $\chi \in (0, 1]$ , the ground state, which has definite spin parity  $P = \pm 1$ , exhibits  $n/2$  transitions  $\pm \rightarrow \mp$  as  $b$  increases from 0, the last one at the factorizing field  $b_s$ . The ground state concurrence changes from antiparallel to parallel just at this last transition. These transitions are, however, appreciable only for  $\chi$  close to 1 (and hence  $b_s$  close to  $b_c$ ) or for small sizes, as otherwise the ground states of both parity sectors are practically degenerate and the concurrence is nearly the same in both states (see Fig. 4) as well as in their mixture. Another consequence of parity conservation is that the exact side limits of  $C_{\pm}$  at  $b = b_s$  are *actually non-zero* and different in finite chains ( $nC_{\pm} \rightarrow \delta/(e^{\delta/2} \pm 1)$ , with  $\delta = n(1 - \chi)$  [33]), being then appreciable for small finite  $\delta$ . In the bottom panel we thus obtain the side limits  $nC_- \approx 1.16$ ,  $nC_+ \approx 0.54$  for the exact result at  $b_s \approx 0.99b_c$ , with  $C_{\pm}$  being in fact *maximum* at  $b = b_s$ .

Fig. 2 depicts the corresponding limit temperatures  $T_L^{\pm}$ , which, remarkably, are also accurately reproduced by the asymptotic MF+RPA result obtained from Eq. (31).  $T_L$  vanishes at  $b = b_s$  but increases  $\forall b > b_s$ , developing thus a separable field window between the antiparallel and parallel concurrences. The bottom panel shows the logarithmic decrease of  $T_L$  with increasing  $n$  in all regions. Let us also remark that the behavior of  $T_L$  bears no relation with that of the mean field critical temperature, Eq. (17), which does not depend on the anisotropy

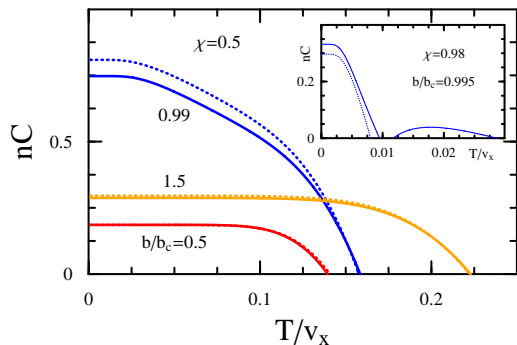


FIG. 3. (Color online) Thermal behavior of the concurrence for  $\chi = 0.5$  and  $n = 100$  at the indicated fields. The inset depicts the non-monotonous behavior just above  $b_s$  for  $\chi = 0.98$  and  $n = 100$ . Solid lines depict exact results, dotted lines those from MF+RPA, Eqs. (22)–(25).

$\chi$  and vanishes for  $b > b_c$ . For  $|b| < b_c$  it is essentially higher than  $T_L$  (except for very low  $n$  [17]), decreasing monotonously from  $\frac{1}{2}v_x$  at  $b = 0$  to 0 at  $b = b_c$ .

For  $\chi = 0.98$ , the exact limit temperature  $T_L^-$  actually exhibits a small *positive slope* close to  $b_s$ , as seen in the top panel (not reproduced by MF+RPA). This entails that at low finite  $T$  the antiparallel concurrence will persist in a narrow region *above*  $b_s$ , while at fixed  $b$  within this region, the thermal behavior of the concurrence will be *non-monotonous*, being first parallel, vanishing and becoming then antiparallel before extinguishing at the final  $T_L^-$ , as depicted in the inset of Fig. 3. Roughly, for small  $b - b_s > 0$ , it is possible to show that  $T_L^\pm \approx \alpha^{-1}(b - b_s)\delta e^{-\delta/2}/(1 - e^{-\delta})$ , with  $\alpha = \ln \coth \delta/4$ , this effect being then noticeable for finite  $\delta = n(1 - \chi)$ .

The different thermal response of  $C$  for fields below, around and above the critical field  $b_c$  can be seen in the main panel of Fig. 3 for  $\chi = 0.5$ . The more rapid decrease with increasing  $T$  for  $b \approx b_c$  is in agreement with Eq. (30), while the results at  $b/b_c = 0.5$  and 1.5 reflect the different decrease rate (Eqs. (23)–(25)).

The origin of the distinct thermal factors in Eqs. (22)–(25) can be seen in Fig. 4, which depicts the excitation energies of the lowest levels ( $S, k^\pm$ ) for  $\chi = 0.5$ . For  $|b| < b_c$ , corresponding levels of opposite parity are practically degenerate. The non-vanishing excitation energies within the maximum spin multiplet are nearly harmonic, the lowest one practically coinciding with the RPA energy (19), whereas the excitation energy of the lowest state with  $S = n/2 - 1$  is almost  $b$  independent and coincident with  $\lambda = v_x$ . The parity degeneracy becomes broken in all levels as  $b$  approaches  $b_c$ , where the maximum spin excitations become low and give rise to the increased thermal sensitivity (Eq. (30)). For  $|b| > b_c$  the RPA energy represents again the lowest excitation energy in the maximum spin multiplet, which has now negative parity, whereas  $\lambda = b + v_z$  is again the excitation of the lowest  $S = n/2 - 1$  state, which has now positive parity.

The corresponding concurrences are shown in the lower

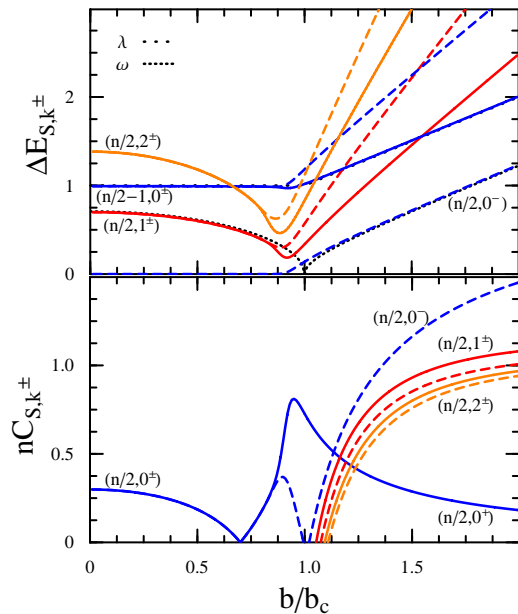


FIG. 4. (Color online) Top: Lowest excitation energies  $\Delta E_{S,k^\pm} \equiv (E_{S,k^\pm} - E_0)/v_x$  for  $\chi = 0.5$  and  $n = 100$ , vs. magnetic field  $b$ .  $E_{S,k^\nu}$  denotes the energy of level  $k$  with total spin  $S$  and parity  $\nu$ , while  $E_0 = E_{n/2,0^+}$ . Solid (dashed) lines depict levels of positive (negative) parity, practically degenerate for  $b < b_c$ . The dotted lines depict the mean field and RPA energies  $\lambda$  and  $\omega$  respectively. Bottom: The corresponding concurrences, including that in the ground state. For  $b < b_c$   $C$  is antiparallel (parallel) for  $b < b_s$  ( $> b_s$ ) in both states  $(n/2, 0^\pm)$ , whereas for  $b > b_c$ , it is parallel in the ground state  $(n/2, 0^+)$  but antiparallel in the other levels depicted.

panel. For  $|b| < b_c$  and  $\chi = 0.5$ ,  $C$  is non-zero just in the degenerate ground states, being almost coincident except for  $b$  close to  $b_c$  and changing both from antiparallel to parallel at  $b_s$ . However, for  $b > b_c$   $C$  is non-zero in all maximum spin states, being parallel in the ground and highest states but antiparallel in the rest. They are essentially the basic states  $|S = n/2, S_z = M\rangle$  plus perturbative corrections. For  $|M| < n/2$  they are already entangled and exhibit hence antiparallel concurrence [23], while for  $|M| = n/2$  the concurrence arises just from the corrections and is hence parallel. We also note that the mixture of the  $n - 1$  states with lower spin  $S = n/2 - 1$  has zero concurrence at all fields (the same occurs with lower spin mixtures) so that it can only decrease the thermal concurrence, which arises then essentially from the ground state, except in anomalous regions (the antiparallel reentry in the inset of Fig. 3 arises from the first excited state).

Finally, Fig. 5 depicts results for a small chain ( $n = 10$ ), where finite size effects become exceedingly important. The stepwise behavior of the exact concurrence at  $T = 0$  is now visible already for  $\chi = 0.5$  (top panel), the side limits at the exact factorizing field  $b_s^{ex} = (1 - n^{-1})b_s$  being non-zero. The MF+RPA result is now less accurate at  $T = 0$ , and leads to the vanishing of  $C_-$  at a field lower

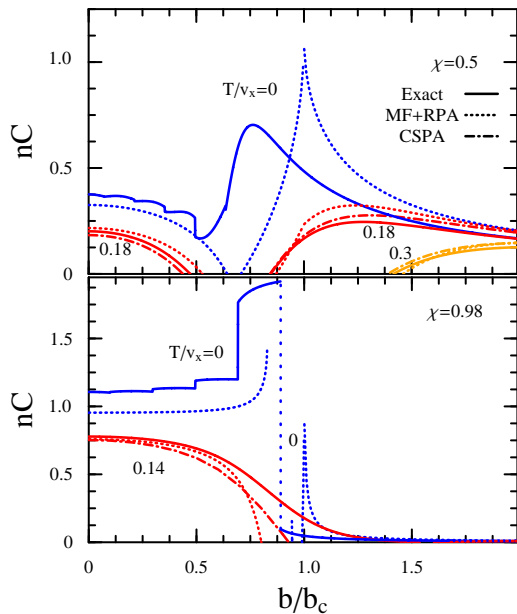


FIG. 5. (Color online) Magnetic behavior of the concurrence for a chain with  $n = 10$  spins at different temperatures, for anisotropies  $\chi = 0.5$  (top) and  $\chi = 0.98$  (bottom). In the latter the antiparallel concurrence increases with increasing field at very low  $T$ , as in the  $XXZ$  case (see text).

than  $b_s$  (and closer to  $b_s^{ex}$ ) if the full expression (A.2) is used for  $C_-$ . Nonetheless, MF+RPA results rapidly improve as  $T$  increases, while the CSPA, although no longer exact, improves again results in the vicinity of  $b_c$ .

When the full square root in the evaluation of  $C_-$  is kept (Eq. (A.2)), the MF+RPA is actually able to qualitatively account for a finite jump in  $C$  for fields close to  $b_s$  but only if  $\chi$  is very close to 1, as seen in the bottom panel. In this case, the MF+RPA result for  $C_-$  at  $T = 0$  does not decrease as  $b$  increases but rather *increases*, in agreement with the exact result, terminating at a final field  $b_f < b_s^{ex}$  where it starts to be complex (and is maximum). For  $\chi = 1 - \delta/n$  and fields just below  $b_c$ , i.e.,  $(b/b_c)^2 = 1 - \varepsilon/n$ , we actually obtain, instead of Eq. (23), the asymptotic MF+RPA expression

$$C_- \approx \frac{1}{n} \left( \frac{1}{2} \varepsilon - \sqrt{\frac{\delta}{\varepsilon}} \coth \frac{1}{2} \beta \omega \right) - 2e^{-\beta v_x} - \frac{1}{n} \left[ 2 \sqrt{\frac{\delta}{\varepsilon}} \coth \frac{1}{2} \beta \omega + \frac{1}{4} \varepsilon (\varepsilon - 4) \right]^{1/2} \quad (34)$$

with  $\omega = \sqrt{\varepsilon \delta} (v_x - v_z)/n$ . While for  $\varepsilon \propto n$  it reduces to Eq. (23), for  $\varepsilon < 4$  it becomes complex if  $\delta$  is sufficiently small. At  $T = 0$ , if  $\delta < \delta_c = \frac{12^3}{5^5} \approx 0.55$ , Eq. (34) becomes complex for  $\varepsilon < \varepsilon_f(\delta) \approx 2.4 + \frac{5}{3} \sqrt{\delta_c - \delta}$ , with  $C_-(b_f) \approx \frac{1}{8} \varepsilon_f^2$ . Note that  $C_-(b_f) > 1$  for  $\delta \lesssim 0.48$ , with  $C_-(b_f) \rightarrow 2/n$  for  $\delta \rightarrow 0$ , which is the correct result for the  $XXZ$  limit [23]. In the case depicted,  $\delta = 0.2$ .

Eq. (34) implies as well that these effects, in particular the increase of  $C_-$  as  $b \rightarrow b_s$  for  $\chi$  close to 1, will disappear for very low  $T \propto \omega \propto b_c/n$ , which is confirmed

in the exact results. One may also appreciate in the bottom panel of Fig. 5 the significant persistence of the antiparallel concurrence up to  $b \approx 1.5b_c$  at  $T/v_x = 0.14$  (not reproduced by MF+RPA or CSPA), which is just the same anomalous behavior discussed in Figs. 2–3, enhanced by the smaller value of  $\delta$ . Nonetheless, even in this extreme case there is a weak but non-zero revival of the parallel concurrence for high fields  $\forall T$  (appreciable in the figure just for  $T = 0$ ) which is correctly reproduced by MF+RPA.

#### IV. CONCLUSIONS

We have analyzed the thermal behavior of the pairwise concurrence in a fully connected spin system with anisotropic couplings placed in a transverse field. For the usual  $1/n$  scaling of coupling strengths, the limit temperature decreases only logarithmically as the size  $n$  increases, and decreases (increases) for increasing field in the antiparallel (parallel) sectors, the latter extending for arbitrarily large fields. This behavior was previously observed for small  $n$  in the temperatures limiting global negativities, for which the pairwise limit temperature provides a lower bound. Anisotropic arrays become then strictly pairwise separable just within a finite field window at any temperature, which collapses into the factorizing field at  $T = 0$ . Remarkably, all previous features of the pairwise entanglement can be captured by a simple thermal MF+RPA treatment, consistently derived from the path integral representation of the partition function, which in the present case is able to provide a reliable analytic description of the concurrence and limit temperature at all fields, exact in the large  $n$  limit. We have also discussed the special finite size effects exhibited by this system for small anisotropies or sizes, whose main aspects can also be qualitatively reproduced by MF+RPA or the full CSPA. These results suggest the possibility of describing by simple means at least the main features of the thermal pairwise entanglement in more complex systems, although the actual accuracy and scope of the RPA in such situations remains to be investigated.

The authors acknowledge support from CIC(RR) and CONICET (JMM, NC) of Argentina.

#### Appendix: MF+RPA Concurrence

We provide here the expressions for the full MF+RPA concurrence derived from Eqs. (3)–(5) and (16). Setting  $v_x = 1$  and  $\tilde{b} \equiv b/b_c$ , in the symmetry breaking phase we



obtain

$$C_+ = -\frac{1-\lambda^2}{2} + \frac{1}{n-1} \left\{ 1 - \frac{\omega}{1-v_y} \coth \frac{1}{2} \beta \omega \left[ 1 + \frac{\zeta}{1-\zeta} \frac{(1-v_y)\lambda^2}{\lambda^2 - \tilde{b}^2} \right] - \left( \frac{\zeta}{1-\zeta} \right)^2 [1 - (3-\zeta)T] \right\}, \quad (\text{A.1})$$

$$C_- = \frac{\lambda^2 - \tilde{b}^2}{2} + \frac{1}{n-1} \left\{ \frac{1 - \tilde{b}^2}{2} - \frac{1-v_y}{\omega} \coth \frac{1}{2} \beta \omega \left[ \frac{\lambda^2 + \tilde{b}^2}{2} + \frac{\zeta}{1-\zeta} \lambda^2 (1-v_z) \right] - \frac{\zeta^2}{(1-\zeta)^2} [1 - (3-\zeta)T] \right\} - \left\{ \left[ \frac{1 + \tilde{b}^2}{2} + \frac{1}{n-1} \left( \frac{1-v_y}{\omega} \coth \frac{1}{2} \beta \omega \frac{\lambda^2 + \tilde{b}^2}{2} - \frac{1 - \tilde{b}^2}{2} \right) \right]^2 - \tilde{b}^2 \left( 1 + \frac{1-v_y}{n\omega} \coth \frac{1}{2} \beta \omega \right)^2 \right\}^{1/2}, \quad (\text{A.2})$$

where  $\zeta = \frac{1}{2}\beta(1-\lambda^2)$  and  $\lambda = \tanh \frac{1}{2}\beta\lambda$ . If  $\tilde{b}$  is not close to 1, we may expand Eq. (A.2) up to  $O(1/n)$  as

$$C_- \approx -\frac{1-\lambda^2}{2} + \frac{1}{n-1} \left\{ 1 - \frac{1-v_y}{\omega} \coth \frac{1}{2} \beta \omega \left[ \frac{\lambda^2 - \tilde{b}^2}{1 - \tilde{b}^2} + \frac{\zeta}{1-\zeta} (1-v_z)\lambda^2 \right] - \frac{\zeta^2}{(1-\zeta)^2} [1 - (3-\zeta)T] \right\} \quad (\text{A.3})$$

For  $\beta\lambda \ll 1$ ,  $\lambda \approx 1 - 2e^{-\beta\lambda}$ , with  $1 - \lambda^2 \approx 4e^{-\beta\lambda}$ . Eqs. (22)–(23) are then obtained from (A.1), (A.3) neglecting  $\zeta$  and setting  $\lambda = 1$  in the  $O(1/n)$  terms. This is correct up to  $O(1/n)$  terms for temperatures where  $C_{\pm}$  are positive, as in such a case  $e^{-\beta\lambda}$  must be  $O(1/n)$ .

Similarly, in the normal phase we obtain

$$C_+ = -\frac{1 - \tanh^2 \frac{1}{2} \beta \lambda}{2} + \frac{1}{n-1} \left\{ 1 - \frac{\omega f_x}{1-f_y} \coth \frac{1}{2} \beta \omega + \frac{1}{2} \zeta \coth \frac{1}{2} \beta \omega \sum_{\mu=x,y} \frac{\omega f_x}{1-f_\mu} \left( \frac{v_\mu}{v_z} - \frac{1}{1-\zeta} \right) - \frac{\zeta}{(1-\zeta)} \frac{3T}{v_z} \right\} \quad (\text{A.4})$$

where  $f_\mu = v_\mu \tanh(\frac{1}{2}\beta\lambda)/\lambda$ ,  $\zeta = \frac{1}{2}\beta v_z (1 - \tanh^2 \frac{1}{2}\beta\lambda)$  and  $\lambda$  determined by Eq. (20). For  $\beta\lambda \ll 1$ ,  $1 - \tanh^2 \frac{1}{2}\beta\lambda \approx -4e^{-\beta\lambda}$ . Eq. (A.4) leads then to Eq. (25) up to  $O(1/n)$  for temperatures where  $C_+ > 0$ , by neglecting  $\zeta$  and setting  $\lambda = b + v_z$  in the  $O(1/n)$  terms.

- 
- [1] M.A. Nielsen and I. Chuang, *Quantum Computation and Quantum Information*, Cambridge Univ. Press, Cambridge, England, (2000).
- [2] C.H. Bennett et al., Phys. Rev. Lett. **70**, 1895 (1993).
- [3] C.H. Bennett and D.P. DiVincenzo, Nature **404**, 247 (2000).
- [4] T.J. Osborne and M.A. Nielsen, Phys. Rev. A **66**, 032110 (2002).
- [5] G. Vidal, J.I. Latorre, E. Rico, and A. Kitaev, Phys. Rev. Lett. **90**, 227902 (2003).
- [6] T. Roscilde, P. Verrucchi, A. Fubini, S. Haas, and V. Tognetti, Phys. Rev. Lett. **93**, 167203 (2004).
- [7] L. Amico, R. Fazio, A. Osterloh and V. Vedral, Rev. Mod. Phys. (2008) (in press).
- [8] S. Popescu, A. Short, and A. Winter, Nature Physics **2**, 754 (2006).
- [9] M.C. Arnesen, S. Bose, and V. Vedral, Phys. Rev. Lett. **87**, 017901 (2001).
- [10] D. Gunlycke, V.M. Kendon, V. Vedral, and S. Bose, Phys. Rev. A **64**, 042302 (2001).
- [11] X. Wang, Phys. Rev. A **64**, 012313 (2001); X. Wang and P. Zanardi, Phys. Lett. A **301**, 301 (2002); X. Wang and Z.D. Wang, Phys. Rev. A **73**, 064302 (2006).
- [12] J. Vidal, G. Palacios, and R. Mosseri, Phys. Rev. A **69** 022107 (2004); S. Dusuel and J. Vidal, Phys. Rev. Lett. **93**, 237204 (2004).
- [13] J. Vidal, G. Palacios, and G. Aslangul, Phys. Rev. A **70** 062304 (2004).
- [14] S. Dusuel and J. Vidal, Phys. Rev. B **71** 224420 (2005).
- [15] J. Vidal, Phys. Rev. A **73** 062318 (2006).
- [16] M. Asoudeh and V. Karimipour, Phys. Rev. A **71**, 022308 (2005).
- [17] R. Rossignoli and N. Canosa, Phys. Rev. A **72**, 012335 (2005). N. Canosa and R. Rossignoli, Phys. Rev. A **73**, 022347 (2006).
- [18] H. J. Lipkin, N. Meshkov, and A. J. Glick, Nucl. Phys. **62**, 188 (1965).
- [19] Y. Makhlin, G. Schön, and A. Shnirman, Rev. Mod. Phys. **73**, 357 (2001).
- [20] J. I. Cirac, M. Lewenstein, K. Mølmer, and P. Zoller, Phys. Rev. A **57**, 1208 (1998).
- [21] S. Hill and W.K. Wootters, Phys. Rev. Lett. **78**, 5022 (1997); W.K. Wootters, Phys. Rev. Lett. **80**, 2245 (1998).
- [22] R. L. Stratonovich, Dokl. Akad. Nauk SSSR **115**, 1097 (1957) (Sov. Phys. Dokl. **2** 458 (1958)); J. Hubbard, Phys. Rev. Lett. **3**, 77 (1959).
- [23] N. Canosa, J.M. Matera, and R. Rossignoli, Phys. Rev. A **76** 022310 (2007).
- [24] A. Werner, Phys. Rev. A **40**, 4277 (1989).
- [25] C.H. Bennett, D.P. DiVincenzo, J.A. Smolin, and W.K. Wootters, Phys. Rev. A **54**, 3824 (1996).
- [26] P. W. Rungta and C. M. Caves, Phys. Rev. A **67**, 012307 (2003).
- [27] A. Fubini, T. Roscilde, M. Tusa, V. Tognetti and P. Verrucchi, Eur. Phys. J. D. **38**, 563 (2006).
- [28] M. Koashi, V. Buzek, and N. Imoto, Phys. Rev. A **62**, 050302(R) (2000); W. Dur, *ibid* **63**, 020303 (2001).
- [29] G. Puddu, P.F. Bortignon, and R. Broglia, Ann. Phys. (N.Y.) **206**, 409 (1991).
- [30] H. Attias and Y. Alhassid, Nucl. Phys. A **625**, 565 (1997).
- [31] R. Rossignoli and N. Canosa, Phys. Lett. B **394**, 242 (2005).



- (1997); N. Canosa and R. Rossignoli, Phys. Rev. C **56**, 791 (1997); R. Rossignoli, N. Canosa, P. Ring, Phys. Rev. Lett. **80**, 1853 (1998).
- [32] J. Kurmann, H. Thomas, and G. Müller, Physica A **112**, 235 (1982).
- [33] R. Rossignoli, N. Canosa, and J.M. Matera (submitted)